IMPACT OF OHMIC HEATING ON MASS TRANSFER IN ELECTROPORATED PLANT TISSUE – INSIGHTS FROM NUMERICAL MODELLING

Samo Mahnič-Kalamiza*, Nataša Poklar Ulrih, Eugéne Vorobiev and Damijan Miklavčič
*Author for correspondence
Faculty of Electrical Engineering
University of Ljubljana,
Ljubljana, Slovenia
E-mail: samo.mahnic-kalamiza@fe.uni-lj.si

ABSTRACT

Electroporation, electropermeabilization or pulsed electric field treatment is the application of electric pulses of sufficient amplitude to target tissue, which entails not only permeabilization of cell membranes, but also heat generation and dissipation, i.e. ohmic heating.

Noticeable rise in temperature has been observed in a number of electroporation applications. The temperature rise is a potential source of alteration of thermodynamic properties of tissue wherein mass transport is occurring. In example, transport parameters such as liquid viscosity and solute diffusivity are temperature-dependent, as they relate to thermodynamic processes.

There is a need to evaluate whether the rate of mass transport is altered significantly by the elevated temperature in plant tissue electroporation. The goal is to advance the basic knowledge of the phenomenon, as well as to optimize further treatment protocols for industrial purposes.

This work presents a theoretical study of thermal relations in tissue immediately following electroporation and begins with a hypothetical spatio-temporal distribution of temperature in a sample of plant tissue as calculated during the course of a simulated electroporation experiment. This step is followed by a mass transfer analysis, where two mathematical models of mass transport in electroporated tissue are used to study the impact of transiently elevated temperature to i) kinetics of diffusion of a test solute, and ii) kinetics of liquid redistribution in tissue and its flow to sample exterior caused by an externally applied pressure.

The main result of the study is a detailed theoretical analysis on the potential influence of heat generated due to the application of electroporation on kinetics of mass transport in tissue. Preliminary theoretical findings of this mass transport study coupled to the heat transfer model indicate that, provided the initial temperature increase in tissue is within reasonable bounds and heat is rapidly conducted away from tissue (i.e. tissue is not thermally insulated), influence of the temperature rise to mass transport in treated tissue is negligible.

INTRODUCTION

An electric field of sufficient strength can cause an increase of conductivity and permeability of the cell membrane. This effect is known as electroporation and is attributed to creation of aqueous pathways in the membrane [1]. Electroporation is essentially the application of electric pulses of sufficient amplitude to cells or target tissue, with the purpose of achieving a permeabilized state of the cell's lipid bilayer membrane.

NOMENCLATURE

c	[mol/m^3]	Solute concentration
c_p	[J/kg.K]	Specific heat capacity
p	[Pa]	Liquid pressure
T	[°C]	Temperature
k_b	[W/m.K]	thermal conductivity (bulk)
k_p,k_e	[m^2]	hydraulic conductivity (pore, tissue extracellular space)
l	[m]	Sample height
h_v	[W/m.K]	Volumetric heat transfer coefficient
R_{cell}	[m]	Cell radius
r	[m]	Radius (pore, solute)
f_c, f_k	[-]	Convection / Permeability correction factors
τ	[-]	Tortuosity of extracellular space
t	[s]	Simulation time
z	[m]	Cartesian axis direction along the primary axis of solute diffusion, heat exchange, or liquid flow
d_m	[m]	Membrane thickness
D_s	[m^2/s]	Solute species *s* diffusion coefficient
f_v	[-]	Tissue volume fraction
f_{por}	[-]	Surface fraction of pores
F	[-]	Cell volume fraction in tissue
G	[Pa]	Compressibility modulus
P_E	[Pa]	Externally-applied pressure (liquid expression model)

Special/Greek characters

τ	[-]	Tortuosity of the extracellular space
ε	[-]	Porosity
η	[Pa.s]	Liquid viscosity (temperature model only)
μ	[Pa.s]	Liquid viscosity (liquid pressure model only)
κ_m	[1/s]	Transmembrane diffusive flow coefficient
α	[-]	Dimensionless proportionality factor reflecting membrane hydraulic conductivity
ρ	[kg/m^3]	Density

Subscripts

b	Bulk (tissue)
amb	Ambient or reference
e	Extracellular
i	Intracellular
δ	Denoting differential temperature, calc. as $T - T_{amb}$
0	Initial value
m	Membrane
p	Pore (except in c_p)

Recently, a model called the dual-porosity model was adapted for the field of electroporation research [2]–[4]

employing mass conservation and transport laws. The model enables coupling effects of electroporation to the membrane of individual cells with the resulting mass transport (and, by extension through analogy, transmembrane heat transfer and heat transfer in tissue). The model leans strongly upon firmly established approaches presented in previous works that are devoted to similar frequent problems in chemical engineering [5], [6]. These approaches in studying mass transport all benefit from a well-known mathematical analogy of heat and mass transfer, and consequently, the developed dual-porosity model is a special case of the classical LaLoThEq (Lack of Local Thermal Equilibrium) model for porous media [7]–[10], which has long been present in literature on heat transfer. An analytical solution has been found for the presented dual-porosity model formulation, however, the model can (and should, through further development) easily be extended with additional dependencies to account for heterogeneities in tissue and temporal component of electroporation, and then solved numerically.

Due to the finite resistance of biological tissue, electroporation unavoidably entails the flow of an electric current through the tissue. This current – through what is electrically an ohmic load – results in heat generation and dissipation, i.e. the effect of ohmic heating. This essentially means that thermal effects are inseparably associated with electroporation. Noticeable rises in temperature have been reported in a number of electroporation applications [11]–[13]. The temperature rise is a potential source of alteration of the thermodynamic properties of the material where mass transport is occurring. Parameters such as viscosity, diffusion rate coefficient, and the rate of chemical reactions and alterations are known to be strongly dependent on temperature, since they are fundamentally related to thermodynamic processes.

This paper presents a theoretical study of mass transport in plant tissue that has been electroporated and also heated due to electroporation via ohmic heating. The tissue is modelled as thermally non-insulated, and rapid dissipation of the generated heat is supposed. We begin with the presentation of a suitable simplified formulation of the thermal conduction model in tissue, not accounting for its heterogeneous structure. The model thus simplified can be considered sufficiently detailed for studying mass transport whose rate has been altered by an augmented temperature in electroporated tissue. The given thermal model is then coupled, via the temperature-dependent mass transport parameters, to the previously developed mass transport models of diffusion and liquid flow during pressing, and results are presented in the form of a parametric study. Due to the coupling of the models, the coefficients of diffusion and viscosity that were previously taken to be constant in the mass transport models, are now arbitrary functions of time. Therefore, it is no longer possible to develop an analytical solution of the thermal model, and the solution must be obtained numerically instead.

The work presented herein is entirely theoretical in nature, based on existing literature and extension of the work done previously in the field of mass transport modelling. Validation and evaluation of suitability of these mathematical formulations is a work in progress and considered out of scope of this paper.

THE HEAT DISTRIBUTION MODEL

In the mass transport study presented in continuation, we look at the effect of transiently elevated temperature on the rate of solute diffusion and liquid flow in electroporated tissue. In order to study this effect of elevated temperature, it is necessary to determine at the outset the spatio-temporal distribution of temperature in tissue.

We suppose that tissue is homogeneously heated (a simplification) due to ohmic heating during electroporation, and we then observe (i.e. simulate) the gradual dissipation of the generated heat out of the sample block of tissue. For the purposes of this study, the tissue samples are all assumed to be cylindrical and of low height as compared to the diameter of the cylinder. This is necessary in order to simplify the three-dimensional model of heat conduction to one dimension, as we are neglecting the heat flow radially and through the side of the cylinder, as the side area is much smaller as compared to the top and bottom surfaces. Figure 1 illustrates this particular geometry.

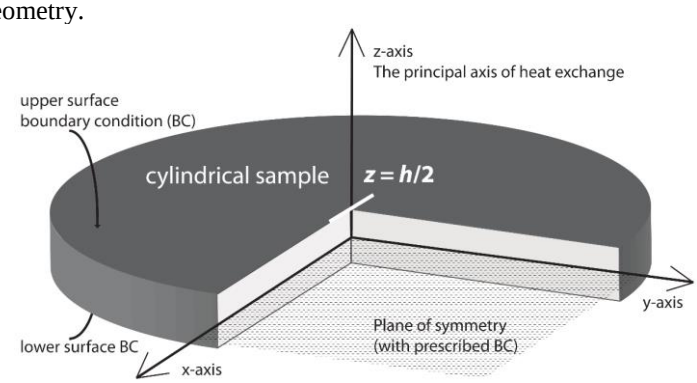

Figure 1 The thermal model geometry – plane of symmetry and boundary conditions. The particular cylindrical geometry of the tissue sample is not significant, but has been used for this illustration for purposes of maintaining consistence with mass transport studies. For the presented schematic to be an adequate representation of the actual state, the sample and setup geometry has to favour thermal transfer along only one (principal) axis.

For the geometry shown in Figure 1 and making one more simplification, i.e. assuming the tissue is homogeneous material, we can propose the following mathematical model – a PDE – for describing the temperature distribution in tissue

$$\frac{\partial T_b}{\partial t} = \frac{k_b}{\rho c_p}\frac{\partial^2 T_b}{\partial z^2} \tag{1}$$

with boundary and initial conditions

$$T_b\big|_{z=h/2} = T_{\text{amb}} \tag{2}$$

$$\left.\frac{\partial T_b}{\partial z}\right|_{z=0} = 0 \tag{3}$$

$$T_b\big|_{t=0} = T_0 \tag{4}$$

where the plane of symmetry ($z = 0$) is located exactly in the middle of the tissue sample of height h at a distance of $h/2$ from either of the sample's largest surfaces, at which the bulk of heat

exchange is taking place (see Figure 1). The index *b* stands for 'bulk', since we have assumed the tissue is homogeneous material instead of composed of multiple phases or spaces (as is the case with mass transport models). In eq. 1–4, t is simulation/experiment time, z is the spatial coordinate along the primary axis of heat conduction, T is the temperature, ρ material density, c_p is the tissue heat capacity, and k_b is the bulk tissue thermal conductivity. All of the physical properties such as density, specific heat capacity and thermal conductivity of the model tissue (apple fruit tissue) used for the parametrical study in continuation can be obtained from literature.

In order to simplify calculations and presentation of results, it is convenient to introduce new variables to observe only temperature differences in relation to the ambient temperature instead of working with absolute values, thus

$$T_{b,\delta} = T_b - T_{amb} \tag{5}$$

This necessitates some corrections to the boundary conditions, which now read

$$T_{b,\delta}\big|_{z=h/2} = T_{\text{amb}} - T_{\text{amb}} = 0 \tag{6}$$

$$\left.\frac{\partial T_{b,\delta}}{\partial z}\right|_{z=0} = 0 \tag{7}$$

and initial condition is henceforth equal to the temperature difference between the absolute and ambient temperature,

$$T_{b,\delta}\big|_{t=0} = T_b\big|_{t=0} - T_{amb} = T_{b0,\delta} \tag{8}$$

In continuation, the introduced δ-notation is kept throughout for clarity and as a reminder; the reader should beware that since T_b was redefined by eq. 5, this same equation should be consulted in order to obtain an absolute value of temperature from its 'δ' counterpart.

Introducing a short-hand variable α in place of the factor $k_b/\rho c_p$, and opening any classical work on heat conduction or mass transfer in solids (e.g. Carslaw & Jaeger, Crank), it is trivial to arrive at an analytical solution of the model, obtaining a spatio-temporal dependence of temperature in tissue for all t and z, namely

$$T_{b,\delta}(z,t) = \frac{4T_{b0,\delta}}{\pi}\sum_{n=0}^{\infty}\frac{(-1)^n}{2n+1}\cos\left(\frac{2n+1}{l}z\right)\exp\left(-\left(\frac{2n+1}{l}\right)^2\frac{k_b}{\rho c_p}t\right) \tag{9}$$

The temperature distribution obtained using eq. 9 can then be used to recalculate the spatial and temporal distribution of mass transport coefficients that are temperature dependent, which will be done in the parametric study in continuation.

THE DIFFUSION PROBLEM

This section presents the already reported on in detail and thoroughly discussed model of dual-porosity for the diffusion problem, the full account of which is given in [3], [4], however here the model is given in its numerical form. This form is necessary in order to facilitate coupling of the theoretical heat distribution model with the mass transport model via temperature-dependent coefficient of diffusion. The coupled model is then used for the theoretical evaluation of the influence of raised temperature in tissue to mass transport for various temperatures (i.e. in a parametric simulation study).

The slightly rearranged fundamental equations of the dual-porosity model for the diffusion problem read

$$\frac{\partial c_e(z,t)}{\partial t} = D_{s,e}\frac{\partial^2 c_e(z,t)}{\partial z^2} + f_v\kappa_m\left(c_i(z,t) - c_e(z,t)\right) \tag{10}$$

$$\frac{\partial c_i(z,t)}{\partial t} = -\kappa_m\left(c_i(z,t) - c_e(z,t)\right) \tag{11}$$

where κ_m here is the transmembrane diffusive flow coefficient.

The appropriate boundary and initial conditions are

$$c_e(t)\big|_{z=l/2} = 0 \tag{12}$$

$$\left.\frac{\partial c_e(t)}{\partial z}\right|_{z=0} = 0 \tag{13}$$

$$c_e(z,0) = c_{e0} \tag{14}$$

$$c_i(z,0) = c_{i0} \tag{15}$$

Strictly adhering to the governing physics behind eq. 10, if the diffusion coefficient $D_{s,e}$ is not space-invariant, eq. 10 must be rewritten into

$$\frac{\partial c_e(z,t)}{\partial t} = \frac{\partial}{\partial z}\left(D_{s,e}(z,t)\frac{\partial c_e(z,t)}{\partial z}\right) + f_v\kappa_m\left(c_i(z,t) - c_e(z,t)\right) \tag{16}$$

which complicates the numerical integration scheme used to calculate c_e.

Using the finite difference approximations of $\partial c/\partial t$ and $\partial c/\partial z$ and the Crank-Nicolson approximation of the temporal derivative by an arithmetic mean of its finite difference representations at the j-th and the (j+1)-th node, it is relatively straightforward (and thus the details are omitted from presentation) to arrive at the finite difference scheme for the extracellular concentration

$$\begin{aligned} &c_{i,j+1}^{(e)} - \frac{r}{4}\left[p_{j+1}c_{i+1,j+1}^{(e)} - q_{j+1}c_{i,j+1}^{(e)} + s_{j+1}c_{i-1,j+1}^{(e)}\right] = \\ &= c_{i,j}^{(e)} + \frac{r}{4}\left[p_j c_{i+1,j}^{(e)} - q_j c_{i,j}^{(e)} + s_j c_{i-1,j}^{(e)}\right] - f_v\kappa_m\delta t c_{i,j}^{(e)} + f_v\kappa_m\delta t c_{i,j}^{(i)} \end{aligned} \tag{17}$$

where

$$p_j = D_{i,j}^{(s,e)} + D_{i+1,j}^{(s,e)} \tag{18}$$

$$q_j = D_{i+1,j}^{(s,e)} + 2D_{i,j}^{(s,e)} + D_{i-1,j}^{(s,e)} \tag{19}$$

$$s_j = D_{i,j}^{(s,e)} + D_{i-1,j}^{(s,e)} \tag{20}$$

and similarly

$$p_{j+1} = D_{i,j+1}^{(s,e)} + D_{i+1,j+1}^{(s,e)} \tag{21}$$

$$q_{j+1} = D_{i+1,j+1}^{(s,e)} + 2D_{i,j+1}^{(s,e)} + D_{i-1,j+1}^{(s,e)} \tag{22}$$

$$s_{j+1} = D_{i,j+1}^{(s,e)} + D_{i-1,j+1}^{(s,e)} \tag{23}$$

This set of eqs. 17–23 can be written in matrix form with the appropriate initial and boundary conditions taken into the account. A similar finite differencing scheme can be written for the intracellular concentration, except that in this case due to absence of a spatial derivative from eq. 11, this scheme is reduced to a simple integration on time and does not necessitate the use of the Crank-Nicolson scheme.

Eqs. 17–23 show that the diffusion coefficient must be known in all spatial and temporal nodes from the plane of independent variables (the z-t plane), and since the diffusion

coefficient is dependent on temperature, the following functional dependence must be known

$$D_{s,e}(z,t) = \frac{f_c}{\tau} D_{s,0}\left(T_{b,\delta}(z,t) + T_{amb}\right) \tag{24}$$

where f_c is the convection correction factor and τ_e the extracellular matrix pathway tortuosity (temperature independent factors) – for details on these parameters, see [3] or [4]. $D_{s,0}$ is the diffusion coefficient of solute species '*s*' in bulk water.

According to the well-known Einstein-Stokes relation [14], the diffusion coefficient in bulk solvent can be (re)calculated from temperature given a known dependence of the solvent viscosity η on temperature

$$D_0(T) = \frac{kT}{6\pi r \eta(T)} = C_0 \frac{T}{\eta(T)} \tag{25}$$

Rather than estimating the diffusion coefficient from solute effective dimensions etc. as demanded by eq. 25, the diffusion coefficient is normally given in form of tabulated data for various solutes at a given temperature. In example, sucrose at 20 °C in water has the diffusion coefficient of about 4.5 10^{-10} $m^2.s^{-1}$ [15]. This holds for 20 °C i.e. at 293 K, and the viscosity of water at this temperature is 1.002 10^{-3} Pa.s [16]. This permits the determination of constant C_0 from eq. 25, which equals $C_0 = D_0(293\ K) \cdot \eta(293\ K) / 293\ K = 1.54\ 10^{-15}\ m^2.Pa.K^{-1}$. This allows for an immediate recalculation of the diffusion coefficient, and several representative values are collected in Table 1 below.

T (°C)	10	20	30	40	50	60	70
$D_{s,0}(T)$ ($\mu m^2.s^{-1}$)	333.7	450.3	584.7	737.0	909.4	1100.5	1310.7
η (μPa.s)	1306.9	1002.0	797.5	653.5	547.1	466.6	403.9

Table 1 Values of the diffusion coefficient of sucrose in an aqueous solution for different temperatures. Recalculated using relation 25 and constant $C_0 = 1.54\ 10^{-15}\ m^2.Pa.K^{-1}$. The corresponding values of viscosity are given alongside for reference, taken from [16].

From values in Table 1 one can calculate that from 10 °C to 70 °C, the diffusion coefficient of sucrose in water increases 4-fold. While this is less than an order of magnitude difference, the diffusion phenomenon is strongly dependent on temperature, since the rate of diffusion $D_{s,e}$ is the most important parameter governing solute extraction kinetics in eq. 16 if the cellular membranes have been permeabilized to a sufficient degree. The values given in Table 1 are used as initial temperatures and the corresponding diffusion coefficients in the parametric study presented in continuation, where the numerical approach to the dual-porosity model of solute diffusion as given in this subsection is used to calculate the $B(t)$ (i.e. normalized Brix) dependence for various initial temperatures of tissue.

Note that the parameter $D_{s,0}$ is also one of the multiplicative factors determining the transmembrane diffusive flow coefficient κ_m, according to eq. 15 given in [4]. Since this parameter is not subject to the spatial derivative, it is much easier to incorporate it into the numerical solution than is the term $D_{s,e}$, and we do not consider the issue further.

In order to calculate $D_0(T)$, which is a spatio-temporal function, i.e. $D_0(T(z, t))$, according to eq. 25 the temperature-dependant viscosity $\eta(T(z, t))$ needs to be determined first. Tabulated data for viscosity such as given in Table 1 can be used in order to obtain a polynomial that can aid in obtaining a high fidelity estimate of viscosity for any temperature within the range of temperatures for which the polynomial fit was calculated. Using the MATLAB (MathWorks, Inc.) function *polyval* and the data in Table 1, one can obtain a fifth-degree polynomial in the form

$$\begin{aligned}\eta(T) = &-1.129\hat{T}^5 - 3.528\hat{T}^4 + 13.006\hat{T}^3 - 23.943\hat{T}^2 + \ldots \\ &+ 83.598\hat{T} - 265.818\hat{T} + 654.000\end{aligned} \tag{26}$$

where $\hat{T}$ is the scaled and centred temperature. Scaling and centring transformation improves the numerical properties of the polynomial and the fitting algorithm. For the above eq. 26, the transformed temperature that can be used to calculate an arbitrary viscosity of water in range of 10 °C to 70 °C is obtained according to the following formula

$$\hat{T} = \frac{T - 313.0000}{21.6025} \tag{27}$$

An additional note on the use of the numerical solution eqs. 17–23. Given a known temperature distribution in the extracellular space, which is equal to the general distribution of temperature in tissue since both the intra- and the extracellular temperatures were assumed not to differ significantly, this temperature distribution (as already given by eq. 9 and reproduced here for reference) is equal to

$$T_{b,\delta}(z,t) = \frac{4T_{b0,\delta}}{\pi} \sum_{n=0}^{\infty} \frac{(-1)^n}{2n+1} \cos\left(\frac{2n+1}{l} z\right) \exp\left(-\left(\frac{2n+1}{l}\right)^2 \frac{k_b}{\rho c_p} t\right) \tag{28}$$

which can be directly inserted into eq. 25 and then $D_{s,0}$ into eq. 24 to obtain values for the diffusion coefficient $D_{s,e}(z, t)$. These values can then immediately be further used in the numerical integration scheme eqs. 17–23. Note that in eqs. 24 and 28, the δ-notation reminds of the use of relative temperature differences in computations, in order to emphasize that for determining the diffusion coefficient, absolute values and not only relative differences in temperature are necessary. In example, for a $T_{e0,\delta}$ of 15 °C, the diffusion coefficient that is sought is the coefficient calculated for the temperature of tissue equal to 35 °C, given the ambient temperature of 20 °C.

THE PRESSING PROBLEM

This section presents the already reported on in detail and thoroughly discussed model of dual-porosity for the pressing problem, the full account of which is given in [4], [17], however, here the model is given in its numerical form. This form is necessary in order to facilitate the coupling of the theoretical heat distribution model with the liquid flow model via temperature-dependent liquid viscosity. This is a prerequisite to theoretical evaluation of the influence of raised temperature in tissue to mass transport for various temperatures in the parametric simulation study that is to follow.

The slightly rearranged fundamental equations of the dual-porosity model for the pressing problem read

$$\frac{\partial p_e(z,t)}{\partial t} = \frac{k_e G_{\varepsilon,e}}{\mu}\frac{\partial^2 p_e(z,t)}{\partial z^2} + \frac{\alpha G_{\varepsilon,e}}{\mu}\left(p_i(z,t) - p_e(z,t)\right) \quad (29)$$

$$\frac{\partial p_i(z,t)}{\partial t} = -\frac{\alpha G_{\varepsilon,i}}{\mu}\left(p_i(z,t) - p_e(z,t)\right) \quad (30)$$

The appropriate boundary and initial conditions are

$$p_e(t)\big|_{z=0} = 0 \quad (31)$$

$$\left.\frac{\partial p_e(t)}{\partial z}\right|_{z=l} = 0 \quad (32)$$

$$p_e(z,0) = p_{e0} \quad (33)$$

$$p_i(z,0) = p_{i0} \quad (34)$$

Strictly adhering to the governing physics behind eq. 29, if the viscosity of liquid η is not space-invariant, eq. 29 must be rewritten into

$$\frac{\partial p_e(z,t)}{\partial t} = \frac{\partial}{\partial z}\left(\frac{k_e G_{\varepsilon,e}}{\mu}\frac{\partial p_e(z,t)}{\partial z}\right) + \frac{\alpha G_{\varepsilon,e}}{\mu}\left(p_i(z,t) - p_e(z,t)\right) \quad (35)$$

Using exactly the same approach as with the diffusion problem, and introducing the following replacements for the sake of algebra

$$\kappa = \frac{k_e G_{\varepsilon,e}}{\mu} \quad (36)$$

$$\upsilon_e = \frac{\alpha G_{\varepsilon,e}}{\mu} \quad (37)$$

$$\upsilon_i = \frac{\alpha G_{\varepsilon,i}}{\mu} \quad (38)$$

we come to the following finite difference Crank-Nicolson scheme for extracellular liquid pressure

$$\begin{aligned} &p_{i,j+1}^{(e)} - \frac{r}{4}\left[\chi_{j+1}p_{i+1,j+1}^{(e)} - \varphi_{j+1}p_{i,j+1}^{(e)} + \vartheta_{j+1}p_{i-1,j+1}^{(e)}\right] = \\ &= p_{i,j}^{(e)} + \frac{r}{4}\left[\chi_j p_{i+1,j}^{(e)} - \varphi_j p_{i,j}^{(e)} + \vartheta_j p_{i-1,j}^{(e)}\right] - \upsilon_e \delta t p_{i,j}^{(e)} + \upsilon_e \delta t p_{i,j}^{(i)} \end{aligned} \quad (39)$$

where

$$\chi_j = \kappa_{i,j} + \kappa_{i+1,j} \quad (40)$$

$$\varphi_j = \kappa_{i+1,j} + 2\kappa_{i,j} + \kappa_{i-1,j} \quad (41)$$

$$\vartheta_j = \kappa_{i,j} + \kappa_{i-1,j} \quad (42)$$

and similarly

$$\chi_{j+1} = \kappa_{i,j+1} + \kappa_{i+1,j+1} \quad (43)$$

$$\varphi_{j+1} = \kappa_{i+1,j+1} + 2\kappa_{i,j+1} + \kappa_{i-1,j+1} \quad (44)$$

$$\vartheta_{j+1} = \kappa_{i,j+1} + \kappa_{i-1,j+1} \quad (45)$$

As in the case of the diffusion problem, the system of equations 39–45 can be written in matrix form with the appropriate initial and boundary conditions taken into the account. A similar finite differencing scheme can also be written for the intracellular liquid pressure, except that in this case due to absence of a spatial derivative from eq. 30, this scheme is reduced to a simple integration on time and does not necessitate the use of a numerical PDE solving scheme.

Since the dependence of viscosity on temperature has been treated in full detail in the preceding section dedicated to the diffusion problem, we do not repeat it at this point. If temperature and therefore viscosity is known for all z, coefficients defined in eqs. 40–45 can be determined and the finite difference scheme applied successively for all t to determine the extra- and intracellular liquid pressure profiles. Integration and scaling to obtain the sample deformation from liquid pressure loss is thereafter a trivial matter, as already presented in detail in [4], [17].

THE PARAMETRIC SIMULATION STUDY

Using the relation 9 or 28 presented in preceding sections, the thermal distribution in a tissue sample can be estimated for the entire duration of a diffusion or pressing experiment. In this parametric study, the time of observation is limited to the first few minutes of the experiment (in contrast to an hour in diffusion and/or pressing experiments). This is due to the rapidly dissipating thermal energy, assuming the tissue sample is heated (by the electric current of electroporation or otherwise) to a temperature above that of the ambient or that of the solution prior to the start of the mass transport experiment/simulation. This thermal energy is rather rapidly dissipated out of the sample tissue block and thus its effects cannot be examined at the same timescales as those of the much slower processes of mass transport. Such an initial temperature increase may however have an important role in mass transport processes immediately after the treatment, i.e. during the first few seconds to minutes. The following parametric study is an attempt at quantifying this influence.

Parameter	Value	Source	Parameter	Value	source
l (m)	0.005	previous experiment	ρ (kg.m^{-3})	1000	water [18]
F (-)	0.345	[4] (apple)	c_p (J.kg^{-1}.K^{-1})	4200	water [18], [19]
R_{cell} (μm)	100	[20]	h_v (W.m^{-3}.K^{-1})	-	not used
k_b (W.m^{-1}.K^{-1})	0.418	[19]	κ_m* (s^{-1})	-	see [4] eq. 15
t_{end} (s)	240	arb. chosen	$T_{i0,\delta}$ (K)	*var.*	arb. chosen
f_v (-)	0.527	F/(1-F)	$T_{e0,\delta}$ (K)	*var.*	arb. chosen
d_m (nm)	5	[3]	f_c (-)	2.5	[4]
τ_e (-)	$\pi/2$	[3]	f_{por} (-)	10^{-6}	[4]
r_s/r_p (-)	0.80	[3], [4]			

Table 2 Parameters used for the parametric study with the dual-porosity model of solute diffusion in an electroporated sample of apple tissue. Note the lower cell volume fraction F due to electroporation. The simulated experiment is for tissue treated according to Protocol A, with 200 V applied to the electrodes. Full details can be found in [4]. *κ_m with units s^{-1} is not thermal conductivity, but the transmembrane diffusive flow coefficient as defined in [3], [4].

The model tissue used for the parametric study was that of apple fruit. For apple fruit tissue, tabulated data can be found in

literature [19], giving the bulk tissue thermal conductivity at room temperature of about 0.418 $W.m^{-1}.K^{-1}$. Other relevant parameters are evident upon inspection of Tables 2 and/or 3.

Using the parameters collected in Table 2 that follow directly from findings presented in [3], [4], simulations using the numerical dual-porosity model for solute diffusion yield results shown in Figure 2a, calculated for a range of tissue temperatures between 10 °C and 70 °C. These simulated kinetics take into the account the reduced (for 10 °C) or increased (for all temperatures > 20 °C, absolute ambient temperature was fixed to 20 °C) diffusion coefficient in electroporated tissue. This increase/decrease is relative to the diffusion coefficient value at the temperature of the ambient, which was the value used in all previous works (i.e. 20 °C).
Figure 2b on the other hand presents simulation results based on the variable viscosity depending on temperature as evaluated by eq. 28, and dual-porosity pressing model results were obtained using the numerical solution given by eqs. 39–45. The range of temperatures in this case was the same, while parameters are collected in Table 3.

Parameter	Value	Source	Parameter	Value	Source
l (m)	0.005	previous exp.	ρ ($kg.m^{-3}$)	1000	water [18]
F (-)	0.345	[4] (apple tissue)	c_p ($J.kg^{-1}.K^{-1}$)	4200	water [18], [19]
R_{cell} (μm)	100	[20]	h_v ($W.m^{-3}.K^{-1}$)	-	not used
k_b ($W.m^{-1}.K^{-1}$)	0.418	[19]	κ_m (s^{-1})	-	see [4] eq. 15
t_{end} (s)	240	arb. chosen	$T_{i0,\delta}$ (K)	*var.*	arb. chosen
f_v (-)	0.527	$F/(1-F)$	$T_{e0,\delta}$ (K)	*var.*	arb. chosen
k_p (m)	$1.25\ 10^{-19}$	[17], [4]	f_k (-)	2.5	[4]
μ (Pa.s)	$f(T_e)$	function of T_e	f_{por} (-)	$4.8\ 10^{-3}$	[4]
G_e (Pa)	$11.0\ 10^5$	[4]			

Table 3 Parameters used for the parametric study with the dual-porosity model of filtration-consolidation (pressing) accounting for variable tissue temperature. Note the lower cell volume fraction F due to electroporation. The simulated experiment is for tissue treated according to Protocol A, with 200 V applied to the electrodes. Full details can be found in [4]. *k_e in m^2 is the extracellular hydraulic permeability, not to be confused with k_b in $W.m^{-1}.K^{-1}$, the thermal conductivity of bulk tissue.

Examining the results in Figure 2a – the diffusion case – one could conclude that the increased or decreased temperature of the tissue does not have a substantial effect on the rate of diffusion. Nevertheless, it would be too early to dismiss the influence of a temperature increase based only on this particular simulated case. The temperature in the simulation drops rapidly due to the small sample thickness and the model representation of an infinitely powerful heat sink/source that is supposed to surround the sample (either liquid solution or electrodes). In case of pressing experiments where metal electrodes are in contact with the tissue sample at all times, this may be a valid approximation. However, in case of the liquid solution in the diffusion example, the finite thermal conductivity of water and its finite quantity cannot be neglected, especially since the tissue bulk thermal conductivity is only slightly below that of bulk water.

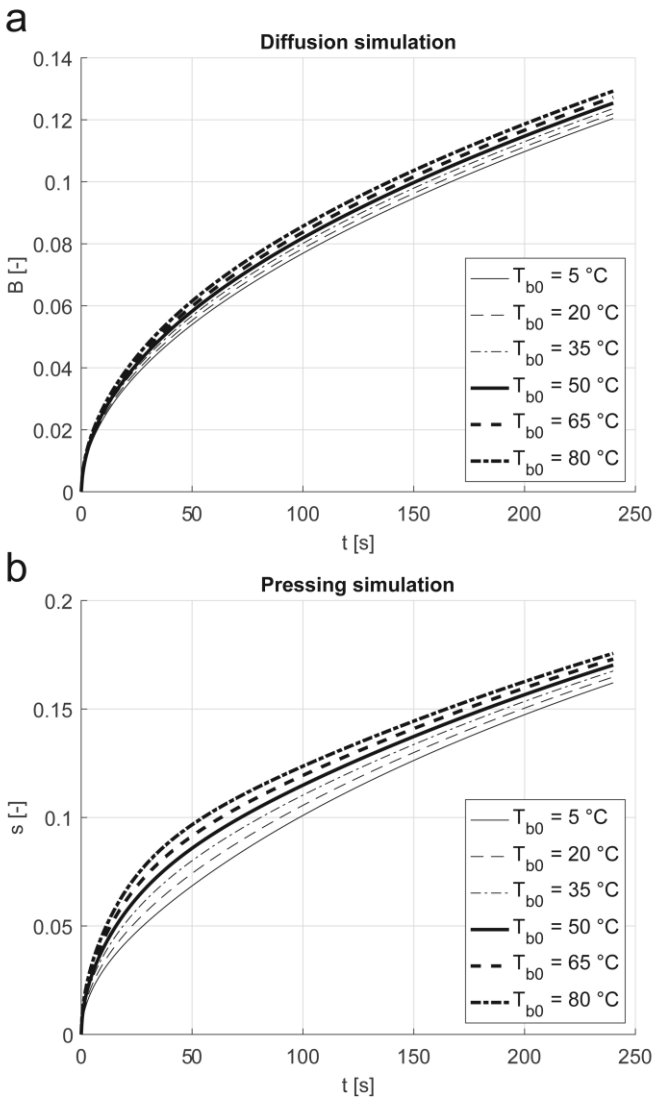

Figure 2 The results of the parametric study for electroporated tissue with the dual-porosity models of solute diffusion (a) and pressing (b) illustrating the effect of temperature-dependent parameters of these models.

The results in Figure 2b clearly demonstrate that initially, during the first four minutes of the simulated pressing experiment, the influence of temperature-dependent viscosity is substantial. However, the effect of decreased viscosity diminishes rather rapidly as temperature drops and viscosity increases, and the end result after four minutes is a discrepancy of only about 10-15 % as compared to ambient temperature,

even for the largest initial increase in temperature that was modelled.

For reasons given above, an important change has to be introduced into the model to account for the finite thermal conductivity in the region exterior to the tissue sample(s). Reconsidering the boundary condition for $z = l/2$, instead of enforcing this boundary condition to 0, one can postulate that the thermal flux entering the interface is equal to the thermal flux exiting the interface (conservation of energy), and is proportional to the temperature difference between tissue and surrounding material (water). The proportionality constant h_s (the tissue-environment heat transfer coefficient) relates this difference in temperatures with the resulting thermal flux, according to the heat exchange properties of the contact tissue-environment.

The boundary condition defined in-line above can be expressed mathematically as

$$\left.\frac{\partial T_b}{\partial z}\right|_{z=l/2^-} = \left.\frac{\partial T_{amb}}{\partial z}\right|_{z=l/2^+} \cong -h_s\left(T_b - T_{amb}\right) \tag{46}$$

and indicates that a positive difference $T_b - T_{amb}$, i.e. a higher tissue sample temperature as compared to that of the ambient, will lead to a negative thermal gradient along the normal vector to the sample surface and in direction of increasing z. The thermal gradient depends on the geometrical properties of the system, which is captured by the heat transfer coefficient h_s. The use of eq. 46 is problematic however, if the surrounding medium is agitated, when there is no thermal gradient in the space outside of the tissue sample. This renders the derivative in eq. 46 identical to zero at $z = l/2^+$, and the derivative (Neumann) boundary condition degenerates to the condition $T_b = T_{amb}$, which is the original Dirichlet boundary condition one was trying to avoid at the outset.

The above dilemma can be easily resolved by ignoring the flux altogether and considering the energy balance instead. If one accounts for the finite thermal capacity of the sample-surrounding medium, which is a valid assumption when the tissue/solution mass ratio is low (valid for laboratory and industrial-scale applications where just enough water is added to grated material to make it pumpable through the treatment chamber), the ambient temperature T_{amb} should also be allowed to increase due to heat leaving the tissue particles and heating the surrounding medium. This means the ambient temperature T_{amb} is now a function of time, however, this is not a problem, since the known thermal distribution in tissue enables precise calculation of the thermal energy dissipated from the sample that was used to heat the environment. One possible approach is thus to determine the total amount of thermal energy leaving the tissue sample by integration, and recalculating (for every time step) the resulting increase in ambient temperature due to this energy. In case the sample and medium density and thermal capacity are assumed identical, the ambient temperature is the following function of tissue temperature

$$T_{amb}(t) = \frac{r_m}{l}\int_0^l \left(T_b(z,t) - T_{b0}\right) dz \tag{47}$$

where r_m is the solid-to-liquid mass ratio, the mass ratio of tissue to the surrounding medium, and l is the sample thickness (along z). Since in all of the analysis thus far, only half of the tissue sample was modelled due to symmetry, the integration boundary has to be corrected, and for hypothetical solid-to-liquid ratio of 1:2 (see diffusion experiments [3]), the ambient temperature changes according to

$$T_{amb}(t) = \frac{2}{2l}\int_0^{l/2}\left(T_b(z,t) - T_{b0}\right) dz = \frac{1}{l}\int_0^{l/2}\left(T_b(z,t) - T_{b0}\right) dz \tag{48}$$

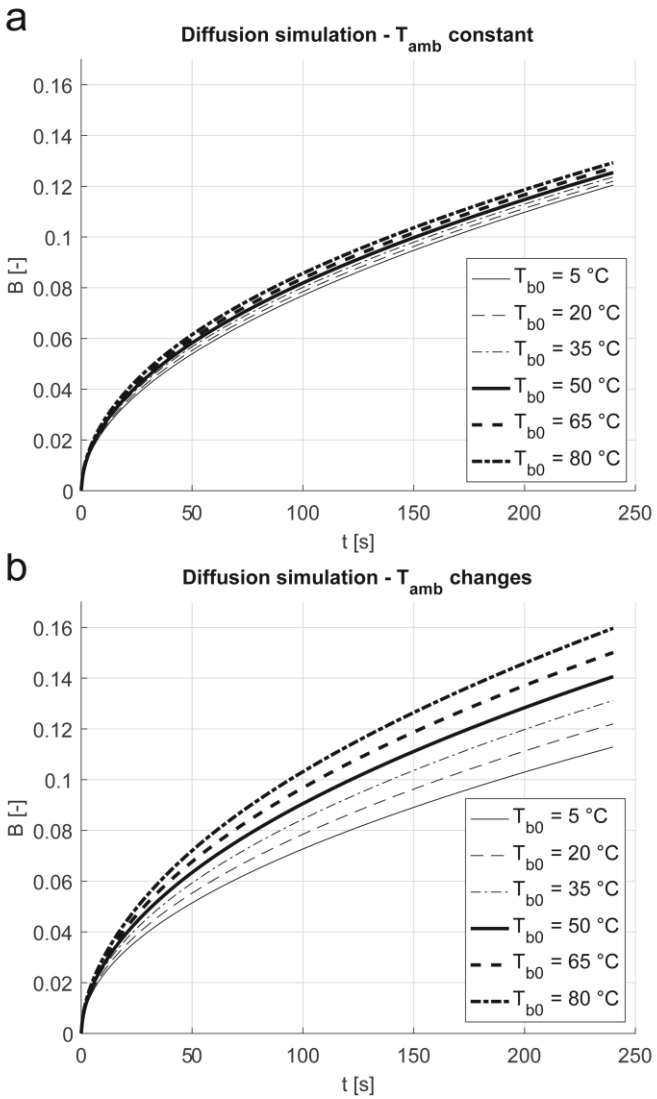

Figure 3 The parametric study of solute diffusion. Without accounting for medium heating (or cooling) (a); and with the medium temperature (T_{amb}) re-calculated at every time step and diffusion coefficient modified accordingly (b).

Note that temperatures in eqs. 47–48 should all be understood as relative and not absolute quantities (refer to the text accompanying eq. 5). Using the ambient temperature dependence eq. 48 into the account in the boundary condition, and simulating using the same system and range of temperatures as used to produce Figure 2a, one obtains results as shown in Figure 3b. Results from Figure 2a were reproduced here again as Figure 3a, but at the same scale along the ordinate axis for easier comparison.

In order to calculate results in Figure 3b, a numerical method of calculating the temperature profile in tissue was used. Note that this causes slight artefacts for small values of *t* if the timescale is divided into equidistant nodes. In this case, a more accurate solution with limited numerical artefacts would have been obtained by use of a logarithmic or otherwise non-linear non-equidistant meshing along the temporal coordinate with finer gradation for small values of *t*. Work concerning this issue extending beyond the basic identification of the problem and illustration by simple simulation as just described, is at this point relegated to future work, and is therefore not further discussed within the scope of the present paper.

The simulated extraction kinetics shown in Figure 3b indicate that in case the more realistic case is modelled where tissue heats (or cools) the medium, the rate of diffusion is more extensively altered as compared to the simulation study where the ambient (medium) is modelled as an ideal sink (or source) of heat. However, since the system of the tissue particles and surrounding medium is not thermally insulated (e.g. in a treatment chamber), the ambient/medium temperature will drop nonetheless and the effect of tissue initial temperature will diminish in time. Also note that only a very substantial increase in tissue initial temperature (e.g. by 30 °C to 60 °C – note that the given temperatures in the legend on Figure 2 or Figure 3 are absolute initial tissue temperatures) is needed to produce a noteworthy increase in the rate of diffusion. Indeed, such temperature increases are reasonably expected to occur in typical experiments or perhaps even industrial applications of pulsed electric field treatment.

To illustrate by an example calculation, consider a resistive disk of tissue, 25 mm in diameter and 5 mm in height, with a resistance of 100 Ω. Its volume is approximately 2.5 cm^3, and its weight equals about 2 g. If the average current of 5 A (at, say, 400 V electrode voltage) flows through the tissue sample during an electric pulse of 100 μs in duration, its maximum dissipative thermal power equals 2 kW. If a thousand such pulses are delivered in a single train with the repetition frequency of 1 kHz, this produces 200 J of thermal energy. If we take, for the specific heat capacity of tissue, the specific heat capacity of water, these 200 J result in an increase in temperature of the 2 g sample by 24 °C.

CONCLUSIONS

This paper examines the relation between tissue temperature, diffusion coefficient and viscosity in two parametric studies where temperature is varied and the effect simulated using the dual-porosity model and its calculated diffusion/expression kinetics. The effect of *constantly* raised temperature was already studied in a similar way in [3], and therefore, in this paper, the approach is taken a step further by considering the influence of temperature if heat is *dissipated* out of tissue during the diffusion stage as realistically expected.

The main conclusion of this paper with relevance to electroporation of tissues is that, given moderate increases in tissue temperature and thermally non-insulated systems permitting sufficiently rapid cooling, the temperature increase itself via augmented diffusion coefficient and reduced viscosity will not have a noteworthy effect on the rate of mass transport. A more important effect to mass transport in the case of elevated temperature is probably the structural alteration of tissue due to synergistic effects between the increased temperature and electroporation, supposing that such effects do exist. We are basing this supposition on the observed temperature-dependent electrical characteristics of tissue (e.g. conductivity) and assuming that electroporation is delivered in a typical treatment protocol comprising a multitude of sequential electric pulses. This hypothesis however remains to be verified by a Multiphysics simulation.

Our findings of the limited impact of elevated temperature to mass transport kinetics should not be misinterpreted by concluding that elevated temperature does not have a strong and direct effect on transport kinetics, but that in most practical cases, thermal dissipation due to electroporation will most likely not be sufficient to noticeably alter mass transport kinetics. This is simply because the electric current-generated heat dissipates too quickly, and the system returns to ambient temperature within seconds or minutes after the treatment.

ACKNOWLEDGEMENTS

The work presented herein was financially supported by the Slovenian Research Agency (ARRS) through research programmes "Biochemical and biophysical characterization of natural compounds (P4-0121)" and "Electroproation-based technologies and treatments (P2-0249)". The laboratory where the work was performed is part of the European Associated Laboratory (LEA) entitled "Pulsed Electric Fields Applications in Biology and Medicine", abbreviated as "LEA EBAM".

REFERENCES

[1] L. Rems and D. Miklavčič, "Tutorial: Electroporation of cells in complex materials and tissue," *Journal of Applied Physics*, vol. 119, no. 20, p. 201101, May 2016.

[2] B. Boyd and S. Becker, "Modeling of In Vivo Tissue Electroporation and Cellular Uptake Enhancement," *IFAC-PapersOnLine*, vol. 48, no. 20, pp. 255–260, Jan. 2015.

[3] S. Mahnič-Kalamiza, D. Miklavčič, and E. Vorobiev, "Dual-porosity model of solute diffusion in biological tissue modified by electroporation," *Biochimica et Biophysica Acta (BBA) - Biomembranes*, vol. 1838, no. 7, pp. 1950–1966, Jul. 2014.

[4] S. Mahnič-Kalamiza, D. Miklavčič, and E. Vorobiev, "Dual-porosity model of mass transport in electroporated biological tissue: Simulations and experimental work for model validation," *Innovative Food Science & Emerging Technologies*, vol. 29, pp. 41–54, May 2015.

[5] A. Halder, A. K. Datta, and R. M. Spanswick, "Water Transport in Cellular Tissues During Thermal Processing," *AICHE J.*, vol. 57, no. 9, pp. 2574–2588, Sep. 2011.

[6] J. L. Lanoiselle, E. I. Vorobyov, J. M. Bouvier, and G. Piar, "Modeling of solid/liquid expression for cellular materials," *AICHE J.*, vol. 42, no. 7, pp. 2057–2068, Jul. 1996.

[7] D. A. Nield, "A note on the modeling of local thermal non-equilibrium in a structured porous medium," *International Journal of Heat and Mass Transfer*, vol. 45, no. 21, pp. 4367–4368, Oct. 2002.

[8] A. Rees, "Microscopic Modeling of the Two-Temperature Model for Conduction in Heterogeneous Media," *JPM*, vol. 13, no. 2, 2010.

[9] P. Vadasz, "Heat Conduction in Nanofluid Suspensions," *J. Heat Transfer*, vol. 128, no. 5, pp. 465–477, Oct. 2005.

[10] P. Vadasz, "On the paradox of heat conduction in porous media subject to lack of local thermal equilibrium," *International Journal of Heat and Mass Transfer*, vol. 50, no. 21–22, pp. 4131–4140, Oct. 2007.
[11] B. Kos, P. Voigt, D. Miklavcic, and M. Moche, "Careful treatment planning enables safe ablation of liver tumors adjacent to major blood vessels by percutaneous irreversible electroporation (IRE)," *Radiol Oncol*, vol. 49, no. 3, pp. 234–241, Sep. 2015.
[12] H. Jaeger, N. Meneses, J. Moritz, and D. Knorr, "Model for the differentiation of temperature and electric field effects during thermal assisted PEF processing," *J. Food Eng.*, vol. 100, no. 1, pp. 109–118, Sep. 2010.
[13] H. Allali, L. Marchal, and E. Vorobiev, "Blanching of Strawberries by Ohmic Heating: Effects on the Kinetics of Mass Transfer during Osmotic Dehydration," *Food Bioprocess Technol.*, vol. 3, no. 3, pp. 406–414, Jun. 2010.
[14] I. Avramov, "Relationship between diffusion, self-diffusion and viscosity," *Journal of Non-Crystalline Solids*, vol. 355, no. 10–12, pp. 745–747, May 2009.
[15] P. W. Linder, L. R. Nassimbeni, A. Polson, and A. L. Rodgers, "The diffusion coefficient of sucrose in water. A physical chemistry experiment," *J. Chem. Educ.*, vol. 53, no. 5, p. 330, May 1976.
[16] J. Kestin, M. Sokolov, and W. A. Wakeham, "Viscosity of liquid water in the range −8 °C to 150 °C," *Journal of Physical and Chemical Reference Data*, vol. 7, no. 3, pp. 941–948, Jul. 1978.
[17] S. Mahnič-Kalamiza and E. Vorobiev, "Dual-porosity model of liquid extraction by pressing from biological tissue modified by electroporation," *Journal of Food Engineering*, vol. 137, pp. 76–87, Sep. 2014.
[18] N. B. Vargaftik, *Handbook of Thermal Conductivity of Liquids and Gases*. CRC Press, 1993.
[19] American Society of Heating, *2006 ASHRAE Handbook: Refrigeration: SI Edition*, SI Edition. ASHRAE, 2006.
[20] F. R. Harker, R. J. Redgwell, I. C. Hallett, S. H. Murray, and G. Carter, "Texture of Fresh Fruit," in *Horticultural Reviews*, J. Janick, Ed. John Wiley & Sons, Inc., 2010, pp. 121–224.